Eur. Phys. J. Special Topics **226**, 765–777 (2017)

DOI: 10.1140/epjst/e2016-60313-6

THE EUROPEAN PHYSICAL JOURNAL SPECIAL TOPICS

Regular Article

Kinetics of ferromagnetic ordering in 3D Ising model: how far do we understand the case of a zero temperature quench?

Subir K. Das[a] and Saikat Chakraborty

Theoretical Sciences Unit, Jawaharlal Nehru Centre for Advanced Scientific Research, Jakkur P.O, Bangalore 560064, India

Received 29 September 2016 / Received in final form 28 November 2016
Published online 5 April 2017

Abstract. We study (nonconserved) phase ordering dynamics in the three-dimensional nearest-neighbor Ising model, following rapid quenches from infinite to zero temperature. Results on various aspects, viz., domain growth, persistence, aging and pattern, have been obtained via Monte Carlo simulations of the model on simple cubic lattice. These are analyzed via state-of-the-art methods, including the finite-size scaling, and compared with those for quenches to a temperature above the roughening transition. Each of these properties exhibit remarkably different behavior at the above mentioned final temperatures. Such a temperature dependence is absent in the two-dimensional case.

1 Introduction

When a paramagnetic system is quenched inside the ferromagnetic region, by a change of the temperature from T_i ($> T_c$) to T_f ($< T_c$), T_c being the critical temperature, it becomes unstable to fluctuations [1–5]. Such an out-of-equilibrium system moves towards the new equilibrium via the formation and growth of domains [1–3]. These domains are rich in atomic magnets aligned in the same direction and grow with time (t) via the curvature driven motion of the interfaces [2,3,6]. The interface velocity scales with ℓ, the average domain size, as [2,6]

$$\frac{d\ell}{dt} \sim \frac{1}{\ell}. \tag{1}$$

This provides a power-law growth [2,6]

$$\ell \sim t^{\alpha}, \tag{2}$$

with $\alpha = 1/2$. Depending upon the order-parameter symmetry and system dimensionality (d), there may exist corrections to this growth law [2].

Apart from the above mentioned change in the characteristic length scale, the domain patterns at different times, during the growth process, are statistically

[a] e-mail: das@jncasr.ac.in

self-similar [2,3]. This is reflected in the scaling property [2],

$$C(r,t) \equiv \tilde{C}(r/\ell), \tag{3}$$

of the two-point equal-time correlation function C, where r $(= |\boldsymbol{r}_1 - \boldsymbol{r}_2|)$ is the scalar distance between two space points and $\tilde{C}$ is a master function, independent of time. A more general correlation function involves two space points and two times, and is defined as [3]

$$C(\boldsymbol{r}_1, t_w; \boldsymbol{r}_2, t) = \langle \psi(\boldsymbol{r}_1, t_w)\psi(\boldsymbol{r}_2, t)\rangle - \langle \psi(\boldsymbol{r}_1, t_w)\rangle\langle \psi(\boldsymbol{r}_2, t)\rangle, \tag{4}$$

where ψ is a space and time dependent order parameter. The total value of the order parameter, obtained by integrating ψ over the whole system, is not time invariant for a ferromagnetic ordering [2]. Thus, the coarsening in this case belongs to the category of "nonconserved" order parameter dynamics [2]. For $\boldsymbol{r}_1 = \boldsymbol{r}_2$, the definition in equation (4) corresponds to the two-time autocorrelation function, frequently used for the study of aging properties [3,7,8] of an out-of-equilibrium system, $t_w (\leq t)$ being referred to as the waiting time or the age of the system. For the two point equal-time case, on the other hand, $t_w = t$. The autocorrelation will henceforth be denoted as $C_{\rm ag}(t, t_w)$. This quantity usually scales as [3,7–12]

$$C_{\rm ag}(t, t_w) = \tilde{C}_{\rm ag}(\ell/\ell_w), \tag{5}$$

where $\tilde{C}_{\rm ag}$ is another master function, independent of t_w, and ℓ_w is the value of ℓ at t_w. Another interesting quantity, in the context of phase ordering dynamics, is the persistence probability P [13–20]. This is defined as the fraction of unaffected atomic magnets (or spins) and decays in a power-law fashion with time as [13]

$$P \sim t^{-\theta}. \tag{6}$$

In the area of nonequilibrium statistical physics, there has been immense interest in estimating the exponents α and θ, as well as in obtaining the functional forms of $\tilde{C}$ and $\tilde{C}_{\rm ag}$, via analytical theories and computer simulations [2,3,13].

In this work, we study all these properties for the nonconserved coarsening dynamics in the Ising model [21],

$$H = -J \sum_{<ij>} S_i S_j, \;\; J > 0, \;\; S_i = \pm 1, \tag{7}$$

via Monte Carlo (MC) simulations [21]. We focus on $d = 3$ and study ordering at $T_f = 0$, for rapid quenches from $T_i = \infty$. This dimension, particularly for $T_f = 0$, received less attention compared to the $d = 2$ case. In $d = 2$, the MC results for $C(r,t)$ are found to be in nice agreement with the Ohta-Jasnow-Kawasaki (OJK) function [2,3,22] (D being a diffusion constant)

$$C(r,t) = \frac{2}{\pi} \sin^{-1}\left[\exp\left(-\frac{r^2}{8Dt}\right)\right]. \tag{8}$$

This expression also implies $\alpha = 1/2$, validity of which has been separately checked [2,3]. For the latter dimension ($d = 2$), in the long time limit, the autocorrelation is understood to scale with x $(= \ell/\ell_w)$ as [7,9,12,23]

$$C_{\rm ag}(t, t_w) \sim x^{-\lambda}, \tag{9}$$

with λ following a lower bound,

$$\lambda \geqslant \frac{d}{2}, \tag{10}$$

predicted by Fisher and Huse (FH) [7]. In this case, also the persistence exponent θ has been estimated [17,18,24,25] for quenches to $T_f = 0$. Furthermore, a few of these aspects, viz., the equal-time correlation function (for large r) and domain growth, are understood to be independent of the value of T_f.

While the above aspects were studied in $d = 3$ as well, our interest in the zero temperature quench in this dimension was drawn by works [26–29] that reported much slower domain growth than the theoretical expectation. Here we mention that below and above the roughening transition temperature (T_R), value of which is nonzero [29] ($\simeq 0.57T_c$) in $d = 3$, there exist differences in structural properties [27]. Above T_R interfaces are rounded and the corresponding width (in equilibrium) logarithmically diverges with the system size. Below T_R, on the other hand, the interfaces are flat and the width has no such system-size dependence. Thus, it may be natural to expect that the dynamics will also be different for $T_f < T_R$ and $T_f > T_R$. As stated above, in this work we study structure and dynamics of coarsening for $T_f = 0$ and compare some of these results with those for $T_f = 0.6T_c$ that lies above T_R. Here note that the coarsening dynamics for $T_f > T_R$ is well understood [5].

The ordering dynamics of $d = 3$ Ising model at $T_f = 0$ were studied by other authors as well [30–33]. Sponge-like structure was reported [32,33] and late time behavior, from simulations of small system sizes, of the domain growth was shown [32,33] to be extraordinarily slow. Our focus here, thus, will be to probe the dynamics over long time without being affected by finite size of the systems. Here we also mention that the zero-temperature late time dynamics of the time dependent Ginzburg-Landau (TDGL) model in this dimension was shown [34] to be consistent with the theoretical expectation. Thus, it is important to establish that Ising model is not different. For experimental results in this context, see reference [5].

While addressing this issue, via simulations with large system sizes over long period, we made further interesting observations in other quantities. In this paper, we present these results on pattern, growth, aging and persistence. While our studies for pattern and aging are new, the results for growth and persistence are presented in forms different from an earlier work [35], to bring completeness to the discussion. It appears, previous conclusions on the value of α was led by the presence of an exceptionally long transient period, which was later hinted in Reference [29]. In the "true" long time limit, the growth exponent is indeed 1/2. Such a trend we observe in the decay of the persistence probability as well. On the other hand, the pattern and aging properties do not seem to exhibit any crossover. These results are very much different from those obtained for quenches to a temperature above the roughening temperature. Such temperature dependence does not exist in the $d = 2$ case. Wherever necessary we presented results from the latter dimension as well.

The rest of the paper is organized as follows. In Section 2 we describe the methods. Results are presented in Section 3. Finally, we conclude the paper in Section 4 by presenting a summary.

2 Methods

All our results were obtained via MC simulations of the Ising model using Glauber spin-flip moves [21,36], where, in each trial move the sign of a randomly chosen spin was changed. Here we use the name Glauber only to emphasize that the trial moves are related to flipping of single spins, to distinguish it from the exchange

moves of Kawasaki, involving pairs of spins, that provide conserved order-parameter dynamics [21]. Algorithm for accepting these moves are described below. For $T_f = 0$, a move was always accepted if it brought a negative change in the energy. Here note that in the zero temperature case moves that bring no change in energy are accepted with different probabilities [32,33], viz., 0, 1/2 and 1, results from which are consistent with each other. In this work we accept such moves with probability 1. On the other hand, for $T_f > 0$, whenever a trial move brought a higher energy contribution, the acceptance was decided by comparing the corresponding Boltzmann factor with a random number (drawn from an uniform distribution), a standard practice followed in the Metropolis algorithm [21]. As stated in reference [21], the conclusions should remain same if one uses the Glauber acceptance algorithm instead.

In $d = 2$ we have used square lattice and for $d = 3$ the results are from simple cubic lattice. All simulations were performed in periodic boxes of volume $V = L^d$, L being the linear dimension of a box, in units of the lattice constant. For this model, the d-dependent critical temperatures [21] are $T_c \simeq 2.269J/k_B$ ($d = 2$) and $T_c \simeq 4.51J/k_B$ ($d = 3$), k_B being the Boltzmann constant. Time in our simulations was measured in units of MC step (MCS), each MCS consisting of L^d trial moves [21]. Unless otherwise mentioned, all results are presented after averaging over at least 10 independent initial configurations, with $L = 512$. For the rest of the paper we set k_B, the lattice constant and the interaction strength (J) to unity.

The average domain size was calculated in two different ways: (i) from the first moment of the domain size distribution $P_d(\ell_d, t)$ as [37]

$$\ell = \int \ell_d P_d(\ell_d, t) d\ell_d, \tag{11}$$

ℓ_d being the distance between two successive interfaces along any direction, and (ii) using the scaling property of the correlation function as [2]

$$C(\ell, t) = 0.1. \tag{12}$$

The average domain size can also be calculated from the first moment of the structure factor (to be introduced later) as well as from the excess energy above the ground state [38]. The results from all these methods should be proportional to each other in the dynamical scaling regime. This fact we have checked by working with a number of methods in other works. Unless otherwise mentioned, presented results in this work are from equation (11). For this purpose, we have eliminated the noise in the configurations at nonzero temperatures, by applying a majority spin rule [37]. Note that the order-parameter ψ here is equivalent to the Ising spin variable S_i. Thus, further discussions on the calculation of the other quantities are not needed since those are clearly understandable from the definitions.

3 Results

We start by showing the plots of ℓ vs t, for $d = 2$ and 3, at $T_f = 0$, on a log-log scale, in Figure 1(a). The system size considered here is comparable to the early studies [26,27] in $d = 3$. The data for $d = 2$ is clearly consistent with the exponent $\alpha = 1/2$, for the whole time range [2,3]. On the other hand, after $t = 10$ the $d = 3$ data appear parallel to $\alpha = 1/3$. For accurate estimation of the exponent for a power-law behavior it is useful to calculate the instantaneous exponent [39]

$$\alpha_i = \frac{d \ln \ell}{d \ln t}, \tag{13}$$

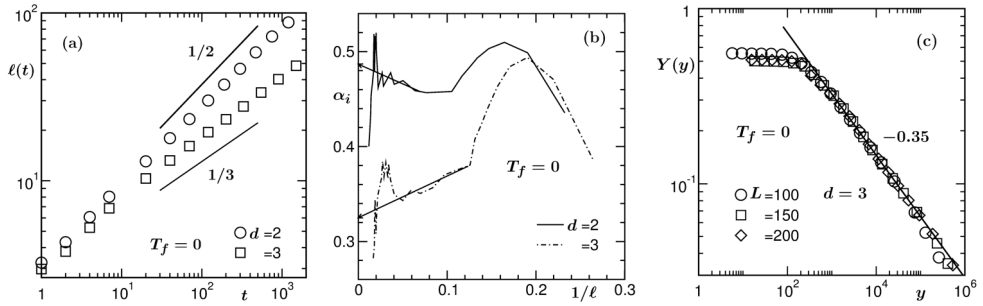

Fig. 1. (a) Log-log plots of the average domain length, $\ell(t)$, vs time, for $T_f = 0$. Results from both $d = 2$ and 3 are presented. In both the cases linear dimension of the system is $L = 200$. The solid lines correspond to two different power-law growths, exponents being mentioned in the figure. (b) Plots of the instantaneous exponent, α_i, vs $1/\ell$, obtained from the data in Figure 1(a). (c) Finite-size scaling exercise for the $d = 3$ results for $\ell(t)$. Here we have shown the scaling function Y with the variation of the dimensionless quantity y. Y was obtained from the best collapse of data from three different system sizes (mentioned in the figure). The solid line corresponds to a power law decay with exponent 0.35. These results are also from $T_f = 0$.

as well as perform finite size scaling (FSS) analysis [21,40]. In Figure 1(b) we plot α_i as a function of $1/\ell$. Clearly, for $d = 3$, the convergence of the data set, in the limit $\ell = \infty$, is consistent with $\alpha = 1/3$, while the $d = 2$ data converge to $\alpha = 1/2$. Since the data for large ℓ in this figure are noisy, to understand the stability of the $d = 3$ exponent over long period, we perform the FSS analysis (see Figure 1(c)). We do not perform this exercise for $d = 2$, since, in this case we have already seen that the data are consistent with the theoretical expectation, as established previously [2,3]. In fact, from here on, unless otherwise mentioned, all results are from $d = 3$ and $T_f = 0$.

In analogy with the critical phenomena [40], a finite-size scaling method in the domain growth problems can be constructed as [37,41,42]

$$\ell(t) = LY(y), \tag{14}$$

where the finite-size scaling function Y is independent of the system size but depends upon y $(= L^{1/\alpha}/t)$, a dimensionless scaling variable. In the long time limit $(y \to 0)$, when $\ell \simeq L$, Y should be a constant. At early time $(y \gg 0)$, on the other hand, the behavior of Y should be such that equation (2) is recovered (since the finite-size effects in this limit are non-existent). Thus

$$Y(y \gg 0) \sim y^{-\alpha}. \tag{15}$$

In the FSS analysis, α is treated as an adjustable parameter. For appropriate choice of α, in addition to observing the behavior in equation (15), data from all different values of L should collapse onto a single master curve. In Figure 1(c) we have used $\alpha = 0.35$. The quality of collapse and the consistency of the power-law decay of the scaling function with the above quoted exponent, over several decades in y, confirm the stability of the value. Thus, it was not inappropriate for the previous studies [26,27] to conclude that the growth is much slower. Nevertheless, given the increase of computational resources over last two decades, it is instructive to simulate larger systems over longer periods [29], to check if a crossover to the theoretically expected exponent occurs at very late time.

In Figure 2(a) we present the ℓ vs t data, on a log-log scale, from a much larger system size [35] than the ones considered in Figure 1. Interestingly, three different

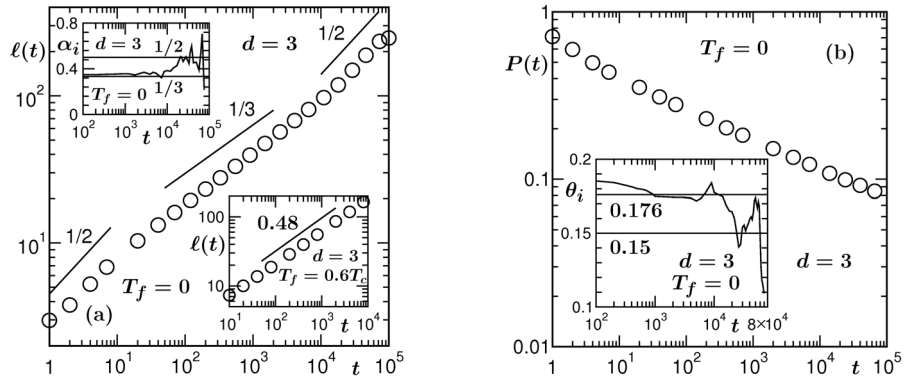

Fig. 2. (a) Log-log plot of $\ell(t)$ vs t, for $d = 3$ and $T_f = 0$, with $L = 512$. The rest of the results are presented for this particular system size. The solid lines indicate different power-law growths, the exponents being mentioned. The upper inset shows instantaneous exponent α_i as a function of t, the x-axis being in log scale, for the data presented in the main frame. The horizontal solid lines there correspond to $\alpha = 1/3$ and $1/2$. The lower inset is same as the main frame but for $T_f = 0.6T_c$. The continuous line there corresponds to a power-law growth with exponent 0.48. (b) Log-log plot of the persistence probability, $P(t)$, as a function of t, for $d = 3$, $T_f = 0$ and $L = 512$. The inset shows corresponding instantaneous exponent, θ_i, vs t, x-axis being in a log scale. The horizontal solid lines there correspond to the ordinate values 0.176 and 0.15. The figure has resemblance with Figure 7(b) of Physical Review E **93**, 032139 (2016).

regimes are clearly visible. A very early time regime shows consistency with $\alpha = 1/2$. This is followed by an exponent $1/3$, that stays for about three decades in time. Finally, the expected $\alpha = 1/2$ behavior is visible, for nearly a decade, before the finite-size effects appear. In this case, an appropriate FSS analysis, to confirm the later time exponent, requires even bigger systems with runs over much longer times, which, given the resources available to us, was not possible. Thus, for an accurate quantification of the asymptotic value of α, we restrict ourselves to the analysis via the instantaneous exponent [39]. In the upper inset of Figure 2(a), we have plotted α_i as a function of t. The quantity shows a nice late time oscillation around the value $1/2$. This is at variance with the data at high temperature. See the ℓ vs t data, on a log-log scale, from $T_f = 0.6T_c$, in the lower inset of Figure 2(a). Here we observe $\alpha \simeq 1/2$ for the whole time range. For this data set as well we avoid presenting results from further analyses. We have not been able to understand the multiple scaling regimes in the $T_f = 0$ data. As mentioned above, for $T_f = 0$, similar results [34] with different regimes were observed in the TDGL model as well.

For $T_f = 0$, the crossover that occurs in the time dependence of ℓ, may be present in other properties as well [35]. These we check next. For the persistence probability, the value of θ was previously estimated [18], also from smaller system sizes, to be $\simeq 0.17$. In Figure 2(b) we show a log-log plot of P vs t and the corresponding instantaneous exponent θ_i (see the inset), calculated as [39]

$$\theta_i = -\frac{d \ln P}{d \ln t}, \tag{16}$$

vs t, for the same (large) system as in Figure 2(a). The early time data is consistent with the previous estimate. At late time there is a crossover [35] to a smaller value $\simeq 0.15$, the crossover time being the same as that for the average domain size. Here note that, despite improvements [16,28,35], the situation with respect to the

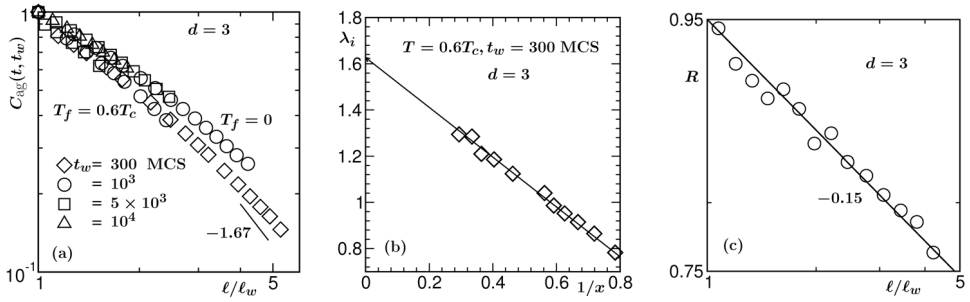

Fig. 3. (a) Log-log plots of the autocorrelation function, $C_{\rm ag}(t,t_w)$, vs ℓ/ℓ_w, for $T_f=0$ and $0.6T_c$. For each value of T_f, results from multiple ages are presented. The solid line corresponds to a power-law decay, exponent for which is mentioned on the figure. (b) Plot of the instantaneous exponent, λ_i, vs $1/x$, for $T_f=0.6T_c$, with $t_w=300$ MCS. The solid line is a guide to the eyes. (c) Log-log plot of the ratio, R, between the master curves for the autocorrelations at $T_f=0.6T_c$ and 0, as a function of x.

calculation of persistence at non-zero temperature may not be problem free, for the reason stated below. Curvature driven coarsening essentially occurs due to flipping of spins in the domain-boundary regions. However, for $T_f>0$, spins inside the domains also flip. Even though the growth mechanism is same, such microscopic dynamics for $T_f>0$, due to thermal fluctuation, affects the calculation of P. To overcome the problem, Derrida [16] proposed simulations of ordered systems as references so that the bulk spin-flips can be appropriately discounted. While we have checked that this method works for T_f close to 0, at very high temperature calculations may still suffer from errors because of interface broadening effect. Thus, for this quantity we avoid presenting results from $T_f=0.6T_c$.

In Figure 3(a) we show the plots of $C_{\rm ag}(t,t_w)$, vs ℓ/ℓ_w, from $T_f=0$ and $0.6T_c$, on a log-log scale, for different values of t_w. Good collapse of data, for both the values of T_f, are visible over the whole range of the abscissa variable. This, in addition to establishing the scaling property of equation (5), implies the absence of the finite-size effects [23,43]. On the issue of the finite-size effects for the nonconserved Ising model, a previous study [23] showed that such effects become important only for $\ell>0.4L$. The length of our simulations were set in such a way that we are on the edge of this limit. For $T_f=0$, this can be appreciated from the ℓ vs t data in the main frame of Figure 2(a). Here note that for conserved Ising model the finite-size effects start appearing when ℓ is approximately 3/4th of the equilibrium domain size limit [37]. Thus, the effects are rather strong here and this fact is consistent with the late time dynamics reported elsewhere [32,33].

From a Gaussian auxiliary field ansatz, in the context of the time dependent Ginzburg-Landau model [2], Liu and Mazenko (LM) [9] constructed a dynamical equation for $C(\boldsymbol{r}_1,t_w;\boldsymbol{r}_2,t)$. For $t\gg t_w$, from the solution of this equation, they obtained (see Eq. (9)) $\lambda\simeq1.67$ in $d=3$. The solid line in Figure 3(a) represents a power-law decay with the above mentioned value of the exponent. The simulation data, for both values of T_f, appear inconsistent with this exponent. Rather, the simulation results on the log-log scale exhibit continuous bending. Such bending may be due to the presence of correction to the power law decay at small values of x. Thus, more appropriate analysis is needed to understand these results.

In Figure 3(b) we plot the instantaneous exponent [9,23,39]

$$\lambda_i=-\frac{d\ln C_{\rm ag}}{d\ln x},\quad x=\frac{\ell}{\ell_w}, \tag{17}$$

as a function of $1/x$, for $T_f = 0.6T_c$. A linear behavior is visible, extrapolation of which, to $x \to \infty$, leads to $\lambda \simeq 1.63$. The latter number follows the FH bound [7] (see Eq. 10)) and is in good agreement with the theoretical prediction of LM [9]. Inserting the linear trend of λ_i in its definition (Eq. (17)), one obtains a full form for the autocorrelation function to be [23]

$$C_{\rm ag} = C_0 \exp\left(-\frac{B}{x}\right) x^{-\lambda}, \tag{18}$$

where C_0 and B are constants. This empirical form was obtained by keeping in mind its usefulness in obtaining an accurate value for λ via finite-size scaling analysis. In fact, such an analysis [23], combining Ising and TDGL models, provided a value 1.68 ± 0.05 which, though closer to the LM one, is slightly higher than a previous estimate [44]. Here note that there already exists [12] a full form, derived from the local scale invariance, for the decay of $C_{\rm ag}$ during coarsening in the ferromagnetic Ising model. Validity of this has been demonstrated in studies [45] of $q(> 2)$-state Potts model. The accuracy of our expression can be justified by comparing it with the latter. However, even though derived from a rigorous theoretical method, this expression contains a large number of unknowns which are not easy to estimate via fitting of the simulation data. In $d = 2$, for which the values of the unknowns were provided by the authors, it has been checked that equation (18) is a reasonable approximation to this.

The decay of $C_{\rm ag}$, as seen in Figure 3(a), for $T_f = 0$ appears slower than that for $T_f = 0.6T_c$. To confirm that, in Figure 3(c) we plot the ratio R, between $C_{\rm ag}$ for $T_f = 0.6T_c$ and $T_f = 0$, on a log-log scale, vs x. Over the whole range of x, that covers pre- as well as post-crossover regimes for domain growth, the data exhibit power-law behavior that can be captured reasonably well by a single exponent $\simeq 0.15$. This implies an absence of crossover in the decay of this quantity and $\lambda \simeq 1.5$, a number significantly smaller than that for $T_f = 0.6T_c$. Irrespective of whether the FH lower bound has actually been violated or not, such small value of λ, compared to the $T_f = 0.6T_c$ case, is an interesting observation which calls for further discussion and calculation of the structural properties. Yeung, Rao and Desai (YRD) made a more general prediction of the lower bound [11], viz.,

$$\lambda \geqslant \frac{d+\beta}{2}, \tag{19}$$

where β is the exponent [46,47] for the small wave-number (k) power-law enhancement of the structure factor (the Fourier transform of $C(r,t)$):

$$S(k) \sim k^{\beta}. \tag{20}$$

Here note that $S(k,t)$ has the scaling form (for a self-similar pattern) [2]

$$S(k,t) \equiv \ell^d \tilde{S}(k\ell), \tag{21}$$

where $\tilde{S}$ is a time independent master function. We call equation (19) a more general lower bound because of the fact that this was derived by keeping both conserved and nonconserved order-parameter dynamics in mind. For nonconserved order parameter [11], as in the present case, $\beta = 0$. Thus the YRD lower bound in this case is same as the FH lower bound. Also note here that originally the FH bound was predicted from the studies of spin-glass systems which later was found to be relevant in coarsening systems like the one considered here, as also was hinted by these authors. The YRD result, on the other hand, was derived by focusing on coarsening in ferromagnets and

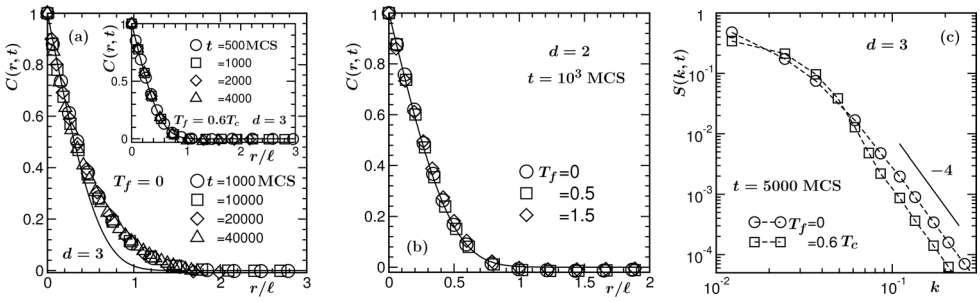

Fig. 4. (a) Scaling plot of the two-point equal time correlation functions from $T_f = 0$ and $d = 3$. The distance along the abscissa has been scaled by the average domain sizes at different times from which data are presented. Inset: same as the main frame, but for $T_f = 0.6T_c$. In both the cases the solid curves represent the OJK form (see Eq. (8)). (b) Scaled correlation functions from different T_f in $d = 2$. The continuous curve is the the OJK function of equation (8). (c) Plots of the structure factors, from $T_f = 0$ and $0.6T_c$, vs k. The solid line represents the Porod law. For both the temperatures, we have presented results from $t = 5000$. These results are from $d = 3$.

multicomponent mixtures. The FH bound can as well be appreciated from the OJK expression for the general correlation function [3,22] of equation (4). This has the form

$$C(r;t,t_w) = \frac{2}{\pi}\sin^{-1}\gamma, \tag{22}$$

with

$$\gamma = \left(\frac{2\sqrt{tt_w}}{t+t_w}\right)^{d/2} \exp\left[-\frac{r^2}{4D(t+t_w)}\right]. \tag{23}$$

For $t = t_w$, this leads to equation (8). For $r = 0$ and $t \gg t_w$, equation (22) provides

$$C_{\rm ag}(t,t_w) \sim \left(\frac{t}{t_w}\right)^{-d/4}. \tag{24}$$

For $\alpha = 1/2$, the exponent in equation (24) provides $\lambda = d/2$, which coincides with the FH lower bound. Since the latter bound is embedded in equation (22) and the violation of it for $T_f = 0$ is a possibility, it is instructive to calculate the structural quantities, viz., $C(r,t)$ and $S(k,t)$, given that equation (22) contains expressions for the latter quantities as well.

In Figure 4(a) we show a scaling plot of $C(r,t)$, vs r/ℓ, for $T_f = 0$, ℓ being extracted from equation (12). Nice collapse is visible for data from wide time range. Given that no crossover in $C(r,t)$ is observed and aging property is strongly related to the structure, it is understandable why a crossover in the autocorrelation is nonexistent. The continuous line in this figure is the OJK function [2,3,22] of equation (8). There exists significant discrepancy between the analytical function and the simulation results. This is expected, given the sponge-like structure [32,33] observed for $T_f = 0$. In the inset of this figure we plot the corresponding results for $T = 0.6T_c$ which, on the other hand, shows nice agreement with equation (8). Here note that in $d = 2$ such temperature dependence does not exist [3]. For the sake of completeness, this we have demonstrated in Figure 4(b). Data from all the temperatures in this case are nicely described by the OJK function.

In Figure 4(c) we show a comparison between the structure factors from $T_f = 0$ and $T_f = 0.6T_c$, in $d = 3$. The k^{-4} line in this figure corresponds to the Porod law [2,3,48] for the long wave-number decay of $S(k,t)$, a consequence of scattering at sharp interfaces like facets at $T_f = 0$. Data from both the temperatures show reasonable consistency with this decay, even in intermediate range of k. For the sake of bringing clarity in the small k region, we did not present the results for the whole range of k. In the smaller wave-number region, disagreement between the slopes in the two cases is visible. This may provide explanation for the small value of λ for $T_f = 0$. For this purpose, below we provide a further discussion on the derivation of YRD. Starting from the equal-time structure factors at t_w and t, YRD arrived at [11]

$$C_{\rm ag}(t,t_w) \leq \ell^{d/2} \int_0^{2\pi/\ell} dk k^{d-1} [S(k,t_w)\tilde{S}(k\ell)]^{1/2}. \tag{25}$$

To obtain the lower bound, they used the small k form for $S(k,t_w)$, as quoted in equation (20). In Figure 4(c) we see that, compared to $T_f = 0.6T_c$, the structure factor for $T_f = 0$ starts decaying at a smaller value of k, providing an effective negative value for β. The latter statement can be further appreciated from the fact that the upper limit of integration in equation (25) is higher for $T_f = 0$ given that average domain size in this case is smaller. This may be the reason for such a small value of λ.

Given that $T_f = 0.6T_c$ lies above the roughening transition temperature, possibility exists [29] that the observed differences between kinetics at the two different values of T_f may be related to this transition [49]. Here note that the results for $T_f = 0.6T_c$ are in agreement with our preliminary results for even higher values of T_f. Systematic studies, however, are needed below T_R to rule out that these are not properties specific to zero temperature, thereby confirming the above mentioned possibility. We mention here, most of the previous studies with nonconserved Ising model focused on $d = 2$, for which there is no non-zero T_R. Furthermore, question remains, why the crossovers, exhibited by the growth of domains and the decay of persistence, are missing in the structure and aging? This fact, e.g. for aging, may have similarity with outcomes from some studies in upper critical dimension. If t and t_w are chosen to be very large, it will be difficult to identify any correction that appears only additively to the leading order scaling form [50,51].

Even though the focus of the paper is on the coarsening dynamics at $T_f = 0$, we would like to further discuss the results for $T_f > 0$. We restate the fact that for nonzero temperature $C(r,t)$ and $\ell(t)$ were calculated after eliminating the thermal noise from the original configurations via a majority spin rule. This exercise essentially makes the interfaces sharp and provides "pure" domain structure in the bulk, facilitating appropriate identification of the domain length by washing out fluctuations at the scale of equilibrium correlation length. Almost perfect match of the OJK function of equation (8) with the simulation data is because of this reason. If the noise is not eliminated, there will be discrepancy in the small r region, reason for deviation from the Porod law in large k limit. This was pointed out by Oono and Puri [52]. The corresponding modified form [4,5,52] of $C(r,t)$ contains a factor $(1 + a\omega^2/t)^{-1}$, appearing in front of the exponential in equation (8), where a is a constant and ω is the interface width. Given that there now exist multiple unknowns, extraction of $\ell(t)$, as well as ω, via fitting of the simulation data (obtained from original configurations) to this modified form, is less reliable. Our noise elimination exercise is performed by keeping such problem in mind. However, the values of $\ell(t)$, obtained from such noise-free configurations, contain ω as well. One important question can now be asked: whether the true domain size should include ω or not. If the answer is in affirmative, all our analyses and conclusions are correct. Otherwise, ω should be appropriately subtracted. Abraham and Upton [53] pointed out that in $d = 3$, above the roughening

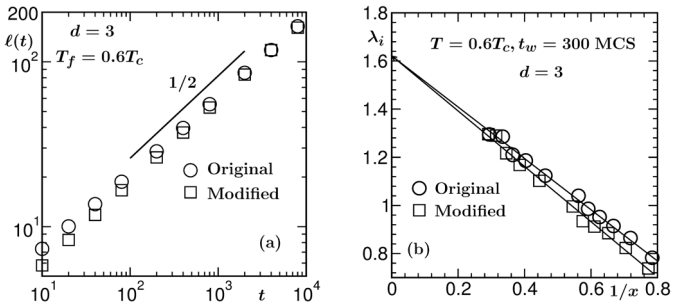

Fig. 5. (a) Log-log plots of ℓ vs t, with (modified) and without (original) subtracting the interface width ($\omega(t)$) from $\ell(t)$. The solid line represents a power-law with $\alpha = 1/2$. (b) Plots of λ_i vs $1/x$ ($x = \ell/\ell_w$) with and without subtracting $\omega(t)$ from ℓ and ℓ_w. The solid lines are guides to the eye. All results correspond to $d = 3$ and $T_f = 0.6T_c$.

transition, $\omega \sim (\ln t)^{1/2}$. Further analyses for $T_f = 0.6T_c$ (in $d = 3$) have been performed by subtracting such logarithmic time dependence of ω from $\ell(t)$. This way, compared to the lower inset of Figure 2 (a), the early time log-log data for ℓ vs t appear more consistent with the exponent $\alpha = 1/2$. Such an exercise, however, does not alter our conclusion on the late time behavior. This is expected, since the (weak) correction is additive. Similar fact we observe in the aging exponent λ. These results are presented in Figure 5 where part (a) contains the data for domain growth and results for λ_i are shown in part (b). In both the cases we have shown comparative pictures between the original and modified analyses. Of course, $T_f = 0$ results do not require any such exercise.

4 Conclusion

We have studied kinetics of phase transition in $3D$ non-conserved Ising model via the Monte Carlo simulations [21], following quench from $T_i = \infty$ to $T_f = 0$. Results are presented for domain growth, persistence probability, aging and pattern, all of which exhibit new features, compared to studies in $d = 2$ and quenches to higher temperature for $d = 3$. The time dependence of the average domain size shows consistency with the expected theoretical behavior only after an exceptionally long transient period [29,35]. This is reflected in the persistence probability [35]. However, no such transient was observed for quenches to a temperature above the roughening transition.

The two-point equal time correlation function does not follow the Ohta-Jasnow-Kawasaki form [22], derived for the nonconserved order-parameter dynamics with scalar order parameter. The latter form, however, is found to be consistent with the simulation data above the roughening transition temperature. Unlike the domain growth and persistence, we did not observe any time dependence (crossover) for this observable. This is reflected in the decay of the autocorrelation function. The latter quantity, at $T_f = 0$, appears to have a power-law decay exponent marginally satisfying the Fisher-Huse lower bound. These results are at deviation with those from $d = 2$ for which there is no non-zero roughening transition.

It will be important to understand the temperature dependence in all these quantities via more systematic studies. This may as well provide improvements in the inputs for the derivation of the OJK function. Furthermore, the reason for long transient in domain growth and persistence deserves attention. These we aim to address in future works.

The authors acknowledge financial support from Department of Science and Technology, India. SKD is grateful to Marie Curie Actions Plan of European Union (FP7-PEOPLE-2013-IRSES Grant No. 612707, DIONICOS) for partial support.

References

1. A. Onuki, *Phase Transition Dynamics* (Cambridge University Press, Cambridge, UK, 2002)
2. A.J. Bray, Adv. Phys. **51**, 481 (2002)
3. S. Puri, V. Wadhawan (eds.), *Kinetics of Phase Transitions* (CRC Press, Boca Raton, 2009)
4. S. Dattagupta, S. Puri, *Dissipative Phenomena in Condensed Matter: Some Applications* (Springer-Verlag, Heidelberg, 2004)
5. M. Henkel, M. Pleimling, *Non-equilibrium Phase Transitions* Vol. 2 (Springer, Netherlands, 2010)
6. S.M. Allen, J.W. Cahn, Acta Metall. **27**, 1085 (1979)
7. D.S. Fisher, D.A. Huse, Phys. Rev. B **38**, 373 (1988)
8. F. Corberi, E. Lippiello, M. Zannetti, Phys. Rev. E **74**, 041106 (2006)
9. F. Liu, G.F. Mazenko, Phys. Rev. B **44**, 9185 (1991)
10. S.N. Majumdar, D.A. Huse, Phys. Rev. E **52**, 270 (1995)
11. C. Yeung, M. Rao, R.C. Desai, Phys. Rev. E **53**, 3073 (1996)
12. M. Henkel, A. Picone, M. Pleimling, Europhys. Lett. **68**, 191 (2004)
13. A.J. Bray, S.N. Majumdar, G. Schehr, Adv. Phys. **62**, 225 (2013)
14. S.N. Majumdar, C. Sire, A.J. Bray, S.J. Cornell, Phys. Rev. Lett. **77**, 2867 (1996)
15. S.N. Majumdar, A.J. Bray, S.J. Cornell, C. Sire, Phys. Rev. Lett. **77**, 3704 (1996)
16. B. Derrida, Phys. Rev. E **55**, 3705 (1997)
17. D. Stauffer, Int. J. Mod. Phys. C **8**, 361 (1997)
18. G. Manoj, P. Ray, Phys. Rev. E **62**, 7755 (2000)
19. B. Derrida, A.J. Bray, C. Godrèche, J. Phys. A **27**, L357 (1994)
20. D. Stauffer, J. Phys. A **27**, 5029 (1994)
21. D.P. Landau, K. Binder, *A Guide to Monte Carlo Simulations in Statistical Physics* (Cambridge University Press, Cambridge, 2009)
22. T. Ohta, D. Jasnow, K. Kawasaki, Phys. Rev. Lett. **49**, 1223 (1982)
23. J. Midya, S. Majumder, S.K. Das, J. Phys.: Condens. Matter **26**, 452202 (2014)
24. T. Blanchard, L.F. Cugliandolo, M. Picco, J. Stat. Mech. P12021 (2014)
25. S. Chakraborty, S.K. Das, Eur. Phys. J. B **88**, 160 (2015)
26. J.G. Amar, F. Family, Bull. Am. Phys. Soc. **34**, 491 (1989)
27. J.D. Shore, M. Holzer, J.P. Sethna, Phys. Rev. B **46**, 11376 (1992)
28. S. Cueille, C. Sire, J. Phys. A **30**, L791 (1997)
29. F. Corberi, E. Lippiello, M. Zannetti, Phys. Rev. E **78**, 011109 (2008)
30. V. Spirin, P.L. Krapivsky, S. Redner, Phys. Rev. E **63**, 036118 (2001)
31. V. Spirin, P.L. Krapivsky, S. Redner, Phys. Rev. E **65**, 016119 (2001)
32. J. Olejarz, P.L. Krapivsky, S. Redner, Phys. Rev. E **83**, 051104 (2011)
33. J. Olejarz, P.L. Krapivsky, S. Redner, Phys. Rev. E **83**, 030104(R) (2011)
34. G. Brown, P.A. Rikvold, Phys. Rev. E **65**, 036137 (2002)
35. S. Chakraborty, S.K. Das, Phys. Rev. E **93**, 032139 (2016)
36. R.J. Glauber, J. Math. Phys. **4**, 294 (1963)
37. S. Majumder, S.K. Das, Phys. Rev. E **81**, 050102 (2010)
38. F. Corberi, M. Zannetti, E. Lippiello, A. Vezzani, arXiv:1506.01199 (2015)
39. D.A. Huse, Phys. Rev. B, **34**, 7845 (1986)
40. M.E. Fisher, in *Critical Phenomena*, edited by M.S. Green (Academic, London, 1971)
41. D.W. Heermann, L. Yixue, K. Binder, Physica A **230**, 132 (1996)
42. S.K. Das, S. Roy, S. Majumder, S. Ahmad, Europhys. Lett. **97**, 66006 (2012)
43. J. Midya, S. Majumder, S.K. Das, Phys. Rev. E **92**, 022124 (2015)
44. M. Henkel, M. Pleimling, Phys. Rev. E **68**, 065101 (R) (2003)

45. E. Lorenz, W. Janke, Europhys. Lett. **77**, 10003 (2007)
46. C. Yeung, Phys. Rev. Lett. **61**, 1135 (1988)
47. S.N. Majumdar, D.A. Huse, B.D. Lubachevsky, Phys. Rev. Lett. **73**, 182 (1994)
48. G. Porod, in *Small-Angle X-ray Scattering*, edited by O. Glatter, O. Kratky, (Academic press, New York, 1982), p. 42
49. H. van Beijeren, I. Nolden, in *Structures and Dynamics of Surfaces II: Phenomena, Models and Methods, Topics in Current Physics*, edited by W. Schommers, P. von Blanckenhagen (Berlin, Springer, 1987), vol. 43
50. M.O. Hase, S.R. Salinas, J. Phys.: Math. Gen. **39**, 4875 (2006)
51. M. Ebbinghaus, H. Grandclaude, M. Henkel, Eur. Phys. J. B **63**, 85 (2008)
52. Y. Oono, S. Puri, Mod. Phys. Lett. B **2**, 861 (1988)
53. D.B. Abraham, P.J. Upton, Phys. Rev. B **39**, 736 (1989)